Polym. Bull.
https://doi.org/10.1007/s00289-018-2382-2

ORIGINAL PAPER

An approximate analytical approach to estimate the diffusivity of toxic chemicals in polymer barrier materials from the time evolution of sessile drop profiles

Molly N. Richards[1] · Michael Bell[2] · Rajagopalan Srinivasan[1] · Ali Borhan[3] · Ramanathan Nagarajan[1]

Received: 28 February 2018 / Revised: 27 April 2018 / Accepted: 21 May 2018

Abstract Any practical technique to determine the diffusivity of chemical warfare agents in protective barrier materials should require handling only miniscule volume of the chemicals and also require data analysis methods that are not computationally burdensome. Such an approach is described here based on imaging the time evolution of ~ 1 µL sessile drop profiles on the barrier surface and using an approximate analytical approach to analyze the time-dependent drop volume and contact angle data for extracting the diffusivity. The approximate analytical approach is validated by comparison against results from computationally intensive finite element simulations available in the literature. The domain of reliable use of the sessile drop technique in terms of the relative importance of the simultaneous evaporation and absorption is assessed using measurements on three challenging toxic chemicals in air and in butyl rubber. The ability of this approach to provide reasonable diffusivity estimates even if the substrate undergoes swelling is explored by studying water sessile drops on a Nafion membrane. The results allow one to conclude that the sessile drop technique coupled to the approximate analytical approach can be reliably used for rapid screening of new barrier materials for protection against chemical warfare agents if the screening is implemented using simulants with low vapor pressures.

Electronic supplementary material The online version of this article (https://doi.org/10.1007/s00289-018-2382-2) contains supplementary material, which is available to authorized users.

✉ Ramanathan Nagarajan
Ramanathan.Nagarajan.civ@mail.mil

[1] Natick Soldier Research, Development and Engineering Center, 15 General Greene Avenue, Natick, MA 01760, USA

[2] Department of Physics, The Pennsylvania State University, University Park, PA 16802, USA

[3] Department of Chemical Engineering, The Pennsylvania State University, University Park, PA 16802, USA

Published online: 31 May 2018

Graphical Abstract

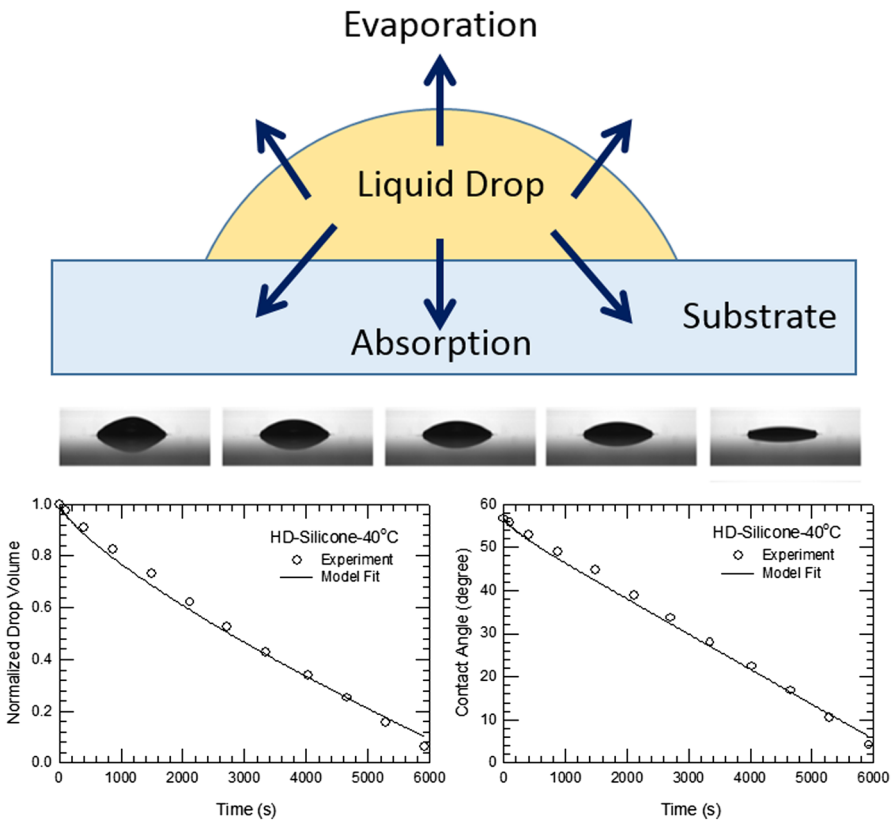

Keywords Sessile drop · Basal radius · Diffusivity of chemical agents · Diffusivity of toxic chemicals · Time evolution of sessile drop profile · Evaporation of sessile drops · Absorption of sessile drops · Model for diffusivity estimation · Diffusivity from contact angle · Barrier polymers

Introduction

Evaluating the diffusivity of chemical agents and highly toxic industrial chemicals in solid substrates is important for the development of protective barrier materials such as gloves, face masks, or soldier uniforms. The diffusivity data are also needed, to assess the extent of contamination when equipment or vehicles with polymer-coated surfaces are subjected to chemical agent attacks or exposed to chemical spillage, and to develop decontamination strategies. The classical approach to determining the liquid diffusivity in a solid is the immersion method wherein the solid substrate is immersed in the liquid chemical of interest and the mass addition

to the substrate from liquid sorption is measured as a function of time [1]. From the immersion method one can obtain both the equilibrium uptake of the liquid into the solid substrate and the diffusivity of the liquid in the substrate. In a typical experiment, the sample is taken out of the immersion bath at specified time intervals, the excess liquid on the surface of the sample is wiped off, the mass of the sample is measured to obtain the amount of liquid absorbed by the substrate, and the sample is then reintroduced into the immersion medium for subsequent time measurements. However, because the procedures for wiping off excess liquid from the surface of the substrate are not well controlled, one cannot avoid inaccuracies in determining the mass of liquid absorbed. Another source of error in this method is that the substrate has to be removed from the immersion bath to allow weighing periodically. Despite such inherent inaccuracies, the immersion method is widely used because of its simplicity and the lack of need for any sophisticated measuring instruments.

Immersion experiments require handling relatively large volumes of liquid, of the order of 10–100 mL. While working with highly toxic chemicals, one would like to avoid handling such large volumes. Colloid science studies on the evaporation of sessile drops (Fig. 1) have shown that using miniscule amounts of liquid of the order of 1 μL, one can estimate its diffusivity in air, by measuring the time evolution of contact angle or volume of the drops [2–11].

Several quantitative models have been developed to characterize the evaporation rate of sessile drops into air considering constant or changing basal radius [3–5], the atmospheric saturation level of the evaporating liquid [5], enhanced evaporation along the contact line of the sessile drop [6], thermal effects due to drop cooling and resultant Marangoni flows [7], and the influence of hydrophobicity or the wettability of the substrate surface [8–10]. These extensive studies on the evaporation of sessile drops have been motivated by the importance of the evaporation phenomenon to applications such as spray drying, fuel injection, inkjet printing, thin film coatings, and manufacturing of novel optical and electronic materials [11].

Willis et al. conducted sessile drop experiments involving the chemical warfare agent HD (bis(2-chloroethyl) sulfide, commonly referred to as mustard) on permeable solid silicone [12], wherein the liquid drop undergoes evaporation into air while also being absorbed into the solid and also on a glass substrate where only

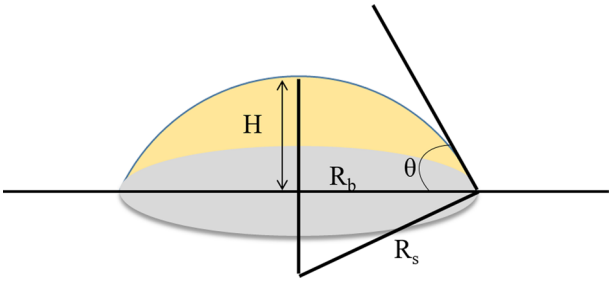

Fig. 1 Spherical cap geometry of the sessile drop. The cap is part of a sphere of radius R_s. Also shown are the basal radius (R_b) which is the contact radius at the solid–liquid interface, apex height (H), and contact angle (θ) of the sessile drop

evaporation occurs [13]. They implemented finite element simulations to solve the mass transport equations governing the evaporation and absorption of the liquid drop, with the liquid–air interface constituting a moving boundary. By fitting the time-dependent volume and/or contact angle from image measurements to the finite element simulations of evaporation on glass [13], they determined the diffusivity D_{SA} for HD in air. Using this estimate for diffusivity in air and by fitting the time-dependent volume and contact angle data on silicone to finite element simulations of simultaneous evaporation and absorption, they determined the diffusivity D_{SR} for HD in silicone.

In this study, an approximate analytical approach to extract diffusivity is presented as an alternative to the computationally intensive numerical simulations of mass transport. This is accomplished by combining the contact angle analysis developed by Hu and Larson (taking into account enhanced mass transfer along the contact line) with the classical analysis of one-dimensional unsteady diffusion of solvent into a semi-infinite solid substrate. On this basis, one obtains explicit analytical expressions for the time rate of change of volume and of contact angle for a sessile drop undergoing both evaporation and absorption. From experimental sessile drop profiles captured by the contact angle goniometer, the basal radius (R_b) and contact angle (θ) at every instant of time are known. Using these variables we calculate the instantaneous drop volume (V) by applying the geometrical relations governing the sessile drop. By fitting the experimental contact angle versus time data and the volume versus time data to the approximate analytical equations for the time rate of change of volume and of contact angle, we determine the unknown diffusivities. The only computational effort involved in this approach is relatively trivial summations and curve fitting that can be performed on any available softwares like Excel, SigmaPlot, etc.

To confirm that the approximate analytical approach provides diffusivity estimates comparable to those obtained by Willis et al. [12, 13] from the finite element mass transport simulations, we have taken their experimental sessile drop data and have analyzed them through analytical equations developed in this work. We have used the experimental data for water on aluminum and for HD on glass [13] to determine the diffusivity D_{SA} in air for water and for HD. We have used the experimental data for HD on silicone [12] to determine the diffusivity D_{SR} for HD in the solid substrate.

The use of sessile drop technique to determine the diffusivity D_{SR} in permeable solids obviously depends on the relative importance of evaporative versus absorptive losses of the liquid, since both processes occur simultaneously. If the evaporative process overwhelms the sorption process, the ability to extract D_{SR} becomes challenging since quantitative measurements of changes due to sorption become relatively very small. We have tested the limits of applicability of the sessile drop technique by studying three chemicals (on aluminum and butyl rubber substrates), whose relative evaporation to absorption behavior departs from the behavior of HD. Based on these studies, we identify the conditions under which the sessile drop technique can be effectively used for estimating diffusivity of industrial toxic chemicals and chemical warfare agents in barrier materials. We also show that apparent diffusivities in complex systems can also be obtained quickly by conducting measurements

of water sessile drops on Nafion membrane, where the transport phenomenon is recognized to be complex because of the swelling of the membrane.

Methods and materials

Experimental setup

The experimental setup consisted of a contact angle goniometer (Biolin Scientific, Theta Tensiometer) with motorized XYZ sample stage and automatic single liquid dispenser (with dispensing resolution of 0.1 μL). An LED-based background light illuminated the droplet for imaging by a high-speed digital camera (0.65 ms–1000 s frame intervals). The experiment was conducted inside a Plexiglas chamber (with internal volume of 213 cm^3) in order to minimize convective effects caused by airflow. To isolate the Theta Tensiometer from any other environmental vibrations, a shock-absorbing Sorbothane sheet (Edmund Scientific) was placed under the feet of the instrument.

Experimental procedure

The toxic chemicals used in this study were tetrachloroethylene (Sigma-Aldrich), trichloroethylene (Alfa Aesar), and acetonitrile (Sigma-Aldrich). Aluminum was used as the impermeable solid substrate in the evaporation study, while butyl rubber was used as the permeable substrate in the absorption experiments. In order to estimate diffusivity of a liquid whose absorption causes the solid to undergo swelling, water on a Nafion membrane (N1110) was used. Contact angle experiments were performed at room temperature (mostly in the range 22–24 °C) with relative humidity varying from 35 to 45%. The data analysis was performed noting the specific temperature and relative humidity corresponding to a given set of measurements.

The camera was regularly calibrated for pixel distance using a machined tungsten carbide sphere (outer diameter 4.000 ± 0.001 mm). The automatic liquid dispensing system was also calibrated regularly. The chemical delivery syringe was filled with the desired liquid, and the tubing and needle were primed with the liquid of interest before testing. A ~ 1-μL droplet (target volume) of the liquid was slowly dispensed and lightly touched off onto the substrate, at which time the image acquisition process was automatically started by the software. Images of the droplet profile were acquired at a rate of 60 frames per second (FPS) for the first minute of testing to ensure the capture of any changes in droplet shape that occurred at the initial instant of droplet deposition. The image capturing rate was decreased to 1 FPS for long timescale imaging.

The three chemicals spread differently on the aluminum substrate, requiring the use of a forced pinning technique for two of the chemicals. The droplet of acetonitrile remained sessile for a considerable time span on the aluminum surface as evaporation occurred. In contrast, tetrachloroethylene and trichloroethylene droplets did not exhibit pinned contact lines on aluminum and spread to a thin film quickly upon

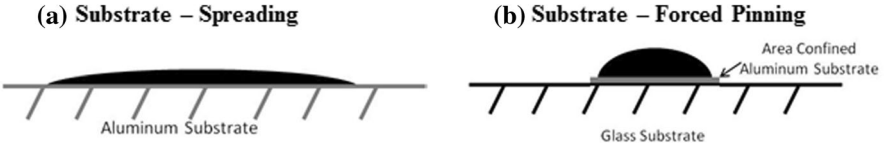

Fig. 2 Schematic of unforced versus forced pinning experimental setup

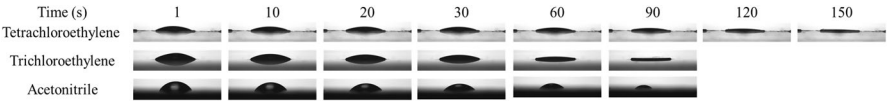

Fig. 3 Typical profile images for acetonitrile, tetrachloroethylene, and trichloroethylene from 1 to 150 s

droplet touch-off. For these two solvents, a technique for pinning the contact line without interfering with the camera was used. A small circular piece of aluminum foil (1/8" in diameter) was used as the substrate, and the droplet (~ 1 µL target) was placed on the foil disk, as shown in Fig. 2, similar to the procedure described by Kelly-Zion et al. [14].

This was done to confine the base of the drop, thereby limiting the amount of spreading that could occur. The droplet contact lines remained pinned at the edge of the aluminum foil disk and did not spread over the edge onto the underlying glass. It should be noted that the size of the foil disk to be used depends on the volume of the drop being used. When the contact line is pinned at the edge of the disk, dispensing additional liquid onto the surface will cause an increase in the contact angle, due to the increase in drop volume. At some point, a further increase in droplet volume can result in the contact angle becoming too large to be supported by the edge of the disk, resulting in the droplet spreading over the glass beyond the aluminum disk. In all of our experiments with the forced contact-line-pinning setup for tetrachloroethylene and trichloroethylene, the droplets remained sessile for a significant amount of time during evaporation.

Experimental data collection

Images of the sessile drop profiles were acquired at specified time intervals. Figure 3 shows the typical side-profile images of the drop taken by the goniometer at various times. The small circular substrate used to pin the tetrachloroethylene and trichloroethylene drops is also visible.

The captured sessile drop images were analyzed using the OneAttension software (Biolin Scientific). The basal diameter (R_b) and contact angle (θ) were directly measured from the captured image. Using these measured values and assuming the spherical cap shape for the drop, the volume V of the droplet was calculated. The captured images were accepted for further analysis as long as the droplet remained sessile to allow measurement of contact angle and basal radius throughout the duration of the experiment and the droplet configuration remained axisymmetric throughout the experiment.

Approximate analytical model

Spherical cap geometry

The spherical cap model is considered to be valid to describe the sessile drop when gravitational effects are negligible [7], as implied by small values of the Bond number, $B_o = \rho g R_o^2/\gamma$, where ρ is the mass density of the liquid, γ is its surface tension, g is the gravitational acceleration, and R_0 is the equivalent spherical radius of the sessile drop. The Bond number provides a measure of the relative importance of the gravitational force compared to the surface tension force. If the Bond number is small, the drop will remain spherical if it is not in contact with a surface and will remain a spherical cap if it is in contact with a surface. For a 1-μL droplet at room temperature (22 °C), tetrachloroethylene, trichloroethylene, and acetonitrile have Bond numbers of 0.193, 0.188, and 0.101, respectively (see Supporting Information S1). The small Bond numbers justify the consideration of spherical cap geometry. Spherical cap geometry was also justified based on the equation developed by Extrand and Moon [15] for the critical drop volume above which the shape of the drop becomes significantly distorted from a spherical cap due to the effect of gravity. Based on that equation (see Supporting Information S1) the critical drop volumes for tetrachloroethylene, trichloroethylene, and acetonitrile at room temperature were estimated to be 4.27, 4.10, and 16.08 μL, respectively, on aluminum substrate and 4.48, 4.10, and 15.22 μL on butyl rubber substrate. Therefore, the assumption of a spherical cap shape for a ~ 1-μL droplet of these chemicals is justified.

For a spherical cap, the basal radius R_b represents the measurable radius of the circular "footprint" of the axisymmetric drop on the substrate, whereas R_s is the radius of curvature of the spherical cap, as shown in Fig. 1. The following geometric relations connect the contact angle θ to other geometrical variables describing the sessile drop.

$$\text{Radius of curvature}: R_s = R_b \csc\theta \tag{1}$$

$$\text{Apex height}: H = R_s(1-\cos\theta) = R_b \csc\theta(1-\cos\theta) \tag{2}$$

$$\text{Air}-\text{liquid surface area}: A(\theta) = 2\pi R_s H = \pi R_b^2 \sec^2(\theta/2) \tag{3}$$

$$\text{Drop volume}: V(\theta) = \frac{1}{3}\pi H^2\left(3R_s - H\right) = \frac{1}{6}\pi R_b^3[3+\tan^2(\theta/2)]\tan(\theta/2). \tag{4}$$

Equations (1) to (4) show that only two independent geometrical features need to be known in order to determine all the geometrical variables associated with the sessile drop. For example, given the basal radius and the contact angle, we can calculate the radius of curvature of the spherical cap from Eq. (1), the apex height from Eq. (2), the surface area of the liquid in contact with air from Eq. (3), and the volume of the sessile drop from Eq. (4).

Model for evaporation alone

For describing the changes in the sessile drop due to evaporation alone, we simply adopt Hu and Larson's [6] equation for the rate of evaporation of a sessile drop. They analyzed the evaporation of a sessile droplet with a pinned contact line experimentally, by analytic theory and by computation using the finite element method, treating the evaporation as a quasi-steady-state process. Therefore, the vapor concentration distribution above the droplet was considered to satisfy the classical Laplace equation, with the recognition that there is a moving liquid–air interface with time. The evaporation flux was found to become strongly singular at the edge of the droplet as the contact angle decreases during evaporation, reflecting the enhanced mass transfer in the vicinity of the contact line. Hu and Larson formulated an analytical expression to represent this effect by empirical fitting of their finite element simulation results. Accounting for this effect, we can describe the change in drop volume due to evaporation, for a sessile drop on an impermeable solid substrate, by

$$\frac{\mathrm{d}V}{\mathrm{d}t} = -\pi R_\mathrm{b}^2 G(\theta) N_\mathrm{S} V_\mathrm{MS}. \tag{5}$$

Here, V_MS is the molar volume of the liquid solvent, N_S is the molar surface flux for a spherical drop of radius R_b (i.e., for a drop with contact angle of $\pi/2$, for which the substrate has no effect on the surface flux by symmetry), and $G(\theta)$ is the geometric correction factor provided by Hu and Larson [6] to account for the non-uniformity in surface flux due to the presence of the solid substrate.

$$G(\theta) = \left(0.27\theta^2 + 1.30\right). \tag{6}$$

Since the timescale for vapor diffusion in air is much smaller than that for drop deformation due to evaporation, the molar flux N_S can be obtained from a quasi-steady-state analysis of vapor diffusion from a spherical cap into stagnant air [16], which yields

$$N_\mathrm{S} = \frac{D_\mathrm{SA}}{V_\mathrm{MA} R_\mathrm{b}} \ln\left(\frac{P - P_{\mathrm{S},\infty}}{P - P_\mathrm{S}^*}\right). \tag{7}$$

Here, P is the system pressure, P_S^* is the saturation pressure of the solvent, $P_{\mathrm{S},\infty}$ is the vapor pressure of the solvent in the ambient air, V_MA is the molar volume of air ($= RT/P$), and R is the universal gas constant ($=0.082$ L atm/mol$^\mathrm{o}$K). Combining Eqs. (5)–(7) and using Eq. (3) for the air–liquid surface area leads to

$$\frac{\mathrm{d}V}{\mathrm{d}t} = -\alpha R_\mathrm{b}\left(0.27\theta^2 + 1.30\right), \quad \text{where } \alpha = \frac{\pi D_\mathrm{SA} V_\mathrm{MS}}{V_\mathrm{MA}} \ln\left(\frac{P - P_{\mathrm{S},\infty}}{P - P_\mathrm{S}^*}\right). \tag{8}$$

Equation 8 is the governing equation for the determination of the diffusivity D_SA in air, using experimental data on the time evolution of the volume of the sessile

drop. Integration of Eq. (8), taking V_o as the initial volume of the drop, provides the instantaneous drop volume, $V(t)$. The integration of Eq. (8) is done using values of instantaneous basal radius $R_b(t)$ and contact angle $\theta(t)$, by a simple summation of difference terms as described in the Supplemental Information S2.

The time rate of change of droplet volume can be related to the time rate of change of contact angle using Eq. (4):

$$\frac{dV}{dt} = \frac{dV}{d\theta}\frac{d\theta}{dt} = \frac{\pi}{4}R_b^3 \sec^4\left(\frac{\theta}{2}\right)\frac{d\theta}{dt}. \tag{9}$$

Combining this relation with Eq. (8), we get the following equation for the time evolution of the droplet contact angle:

$$\frac{d\theta}{dt} = -\frac{4\alpha}{\pi R_b^2}\left(0.27\theta^2 + 1.30\right)\cos^4\left(\frac{\theta}{2}\right). \tag{10}$$

Equation 10 is the governing equation for the determination of the diffusivity in air, D_{SA}, using experimental data on the time evolution of the contact angle. Integration of Eq. (10), taking θ_o as the initial contact angle of the drop, provides the instantaneous contact angle $\theta(t)$. The integration of Eq. (10) is done using experimental measurements of instantaneous basal radius $R_b(t)$ and the contact angle $\theta(t)$, as a summation as described in Supplemental Information S2. The instantaneous $V(t)$ obtained from integration of Eq. (8) and the instantaneous contact angle $\theta(t)$ obtained from the integration of Eq. (10) can be simultaneously fitted to the measured $V(t)$ and $\theta(t)$, to obtain the estimate of the diffusivity in air, D_{SA}.

It should be noted that even though instantaneous values of $R_b(t)$ are used in Eqs. (8) and (10), we suggest that the approximate analysis be performed only if the increase in the basal radius does not exceed 50% of the initial basal radius. This data acceptance criterion is proposed in order to ensure that the contact angle measurements from the imaging software are reliable. Increased spreading or even complete wetting results in very low contact angles of which the software cannot differentiate with confidence. For all of the systems considered in this work, this criterion was met, and all measured values of $R_b(t)$ were used.

Model for simultaneous evaporation and absorption

For simultaneous evaporation into air and absorption in a permeable solid substrate, the time rate of change of the droplet volume may be written by adding to Eq. (8), the contribution to account for the absorption. The absorption term is obtained by considering one-dimensional unsteady diffusion of solvent into an isotropic semi-infinite solid substrate. For adsorption into a semi-infinite medium, when the surface is maintained at a constant solvent concentration, Crank [17] has provided an expression for the total moles per unit area M_{abs} taken up at time t to be

$$M_{abs} = 2C_o\left(\frac{D_{SR}t}{\pi}\right)^{1/2}. \tag{11}$$

Here, D_{SR} is the solvent diffusivity in the solid and C_o is the surface concentration of the solvent within the solid, which is the saturation concentration since the surface is in contact with the liquid solvent. Multiplying both sides of Eq. (11) by the molar volume V_{MS} of the solvent and by the contact area of the liquid with the surface, we get the total volume V_{abs} taken up by the solid at time t.

$$V_{abs} = M_{abs} V_{MS} \pi R_b^2 = 2 C_o V_{MS} \pi R_b^2 \left(\frac{D_{SR} t}{\pi} \right)^{1/2} = 2 \phi_S \pi R_b^2 \left(\frac{D_{SR} t}{\pi} \right)^{1/2}. \quad (12)$$

Here, we have recognized $C_o V_{MS}$ to be the volume fraction of the solvent in the solid, ϕ_S, at saturation conditions. The time rate of change of the volume absorbed is given by the derivative of Eq. (12) with respect to time. We add this absorption contribution to the contribution from evaporation defined in Eq. (8) to get the total change in sessile drop volume due to the simultaneous evaporation and absorption to be

$$\frac{dV}{dt} = -\alpha R_b \left(0.27\theta^2 + 1.30 \right) - \pi R_b^2 \phi_S \left(\frac{D_{SR}}{\pi t} \right)^{1/2}. \quad (13)$$

The first term on the right-hand side represents the evaporation contribution that we have already discussed, and the second term represents the absorption contribution generated from Eq. (12). The value of D_{SA} in the evaporation term (appearing within α) is set equal to the estimate obtained from the evaporation-only data (i.e., from experiments with the same solvent on an impermeable solid). This leaves two unknown parameters in the absorption model—namely ϕ_S and D_{SR}. Since the unknowns appear together in Eq. (13), only the product $\phi_S^2 D_{SR}$ can be estimated by fitting the absorption data. To estimate D_{SR}, the value of the partition coefficient ϕ_S must either be known or be obtained through independent equilibrium measurements. Alternately, one can simply use $\phi_S^2 D_{SR}$ as the metric of solvent permeation through the solid since it conveniently combines both the equilibrium (ϕ_S) and the kinetic (D_{SR}) measures of mass transport.

Combining Eq. (4) with the governing equation for the time evolution of droplet volume (Eq. 12), we can obtain the following equation for the time evolution of contact angle.

$$\frac{d\theta}{dt} = -\frac{4}{\pi R_b^2} \cos^4\left(\frac{\theta}{2} \right) \left[\alpha \left(0.27\theta^2 + 1.30 \right) + \pi R_b \phi_S \left(\frac{D_{SR}}{\pi t} \right)^{1/2} \right]. \quad (14)$$

On integrating Eqs. (13) and (14), with the initial conditions V_o and θ_o, respectively, we obtain the instantaneous values $V(t)$ and $\theta(t)$ which are then fitted to the measured values, to obtain estimates of $\phi_S^2 D_{SR}$.

Allowing for changing basal radius

A key assumption in many existing evaporation models, including the work of Hu and Larson we have adopted, is that the contact line remains pinned, or in other words, the basal radius of the drop (R_b) remains constant. The finite element simulations of mass transport have been implemented with the constraint of a constant basal radius [12, 13]. Experiments indicate that the basal radius may not remain constant, although the changes may be small or large in different systems depending on the liquid and the solid substrate. As part of our approximate approach, we allow for changes in basal radius in our data analysis. In our approach, measurements of the instantaneous basal radius and contact angle were used to calculate the instantaneous drop volume. This drop volume versus time data and the contact angle versus time data were then fitted to the evaporation only and the simultaneous evaporation/absorption models. This approach allowed us to extract diffusivities from experimental data, whether or not the basal radius remains strictly constant, decreases, or increases. As mentioned before, we accept data for analysis only if the increase in the basal radius does not exceed 50% of the initial basal radius to ensure the image analysis by the contact angle goniometer is reliable.

Results and discussion

Comparing results from approximate analytical approach against finite element simulations

To compare the estimates for diffusivity in air obtained from the approximate analytical approach against those from the finite element simulations [13], we start from a common sessile drop experimental data. The normalized sessile drop volume versus time data for water on glass given in Fig. 4 and for HD on glass substrate given in Fig. 6 of Ref. [13] were used as the data for analysis. The actual volume of the sessile drop was kept close to, but not necessarily exactly at, the target volume of 1 μL in these experiments. Since the variation from the target volume was reported to be not large, the initial droplet volume was taken to be 1 μL for determining the actual volume versus time data. The $V(t)$ versus t data were converted to contact angle versus time data, using Eq. (4) for the spherical cap geometry, taking the basal radius to be constant and having the values (0.92, 0.8, and 0.92 mm) for water at the three temperatures of 20, 40, and 60 °C; 1.11, 1.12, and 1.13 mm for HD at 20, 40, and 50 °C, respectively.

For evaporation studies on water, the vapor pressure of water, $P_{S,\infty}$, in the ambient air was determined from the relative humidity (R_H) and the saturation vapor pressure (P_S^*) as

$$P_{S,\infty} = \left(\frac{R_H}{100}\right) P_S^*. \tag{15}$$

For the water experiments in Ref. [13], the R_H values were specified to be 39.1, 18.1, and 1.5% at 20, 40, and 60 °C, respectively. The saturated vapor pressure, P_S^* in

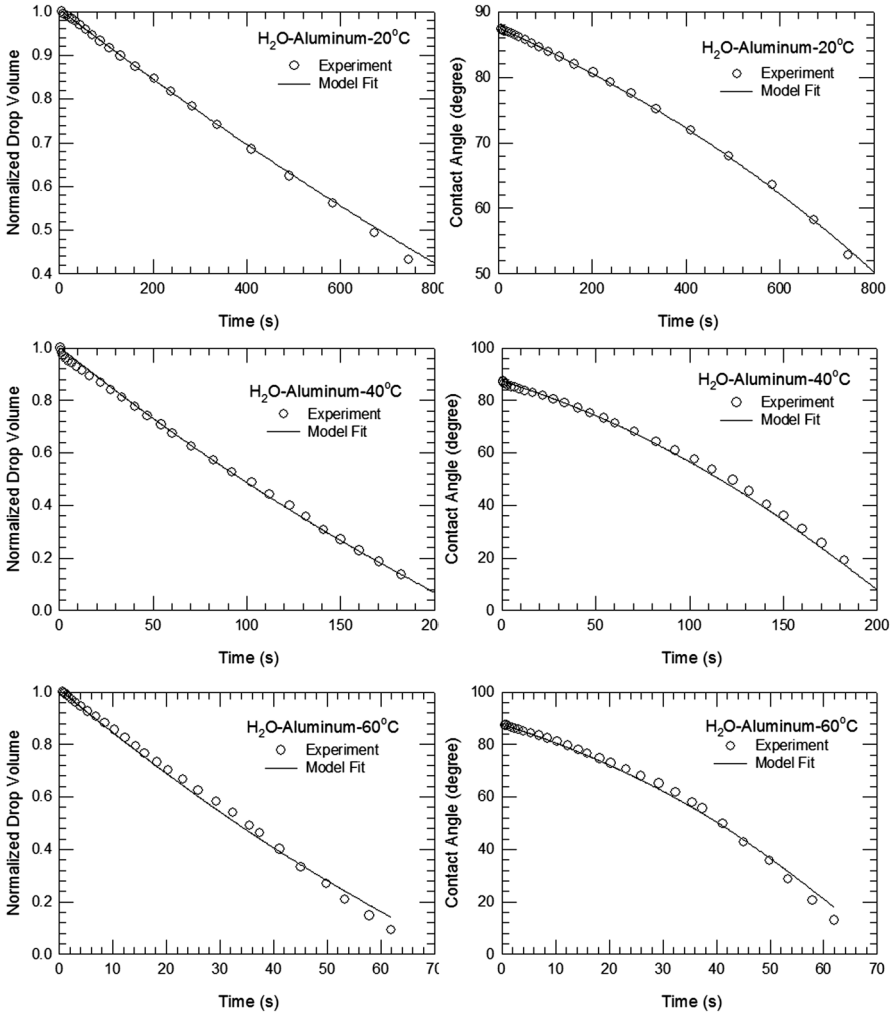

Fig. 4 Model fits of volume versus time and contact angle versus time data for water on aluminum at three temperatures (20, 40, and 60 °C). The experimental data are from Willis et al. [13]

torr, of water and HD (as well as of all other solvents in this study) were estimated using the classical Antoine equation,

$$\log_{10} P_{\mathrm{S}}^{*} = A - \frac{B}{C + T}, \tag{16}$$

with T in °C. The Antoine constants A, B, and C for all solvents [18] are listed in Table S2 of Supporting Information S2. For all solvents in this study other than water, the vapor pressure of the solvent in ambient air was $P_{\mathrm{S},\infty} = 0$.

The diffusivities estimated from sessile drop measurements were also compared against estimates derived from the Fuller–Schettler–Giddings (FSG) equation, a widely used empirical correlation in the literature [19].

$$D_{SA}^{FSG} = \frac{10^{-3}T^{1.75}}{P\left[\left(V_{A,atom}\right)^{1/3} + \left(\sum V_{S,atom}\right)^{1/3}\right]^2}\left(\frac{1}{M_S} + \frac{1}{M_A}\right)^{1/2}. \tag{17}$$

In this equation, T is the temperature in Kelvin, P is the system pressure in atm, M_S is the molecular weight of the solvent, M_A is the molecular weight of air (29 g/mole), $\Sigma V_{S,atom}$ is the atomic diffusion volume of the solvent calculated using group contributions provided with the FSG equation [19], and $V_{A,atom}$ is the atomic diffusion volume for air (20.1 cm^3/mol) [19]. Table S2 of Supporting Information S2 lists the diffusion volumes of the solvents used for estimating diffusivities in air from the FSG equation.

Figure 4 shows the fits of experimental sessile drop volume versus time data to the integrated volume based on Eq. (8) and also the fits of the experimental sessile drop contact angle versus time data to the integrated contact angle based on Eq. (10) for water, at three temperatures. The integrations were performed by simply summing the difference terms over time intervals (as described in Supplemental Information S3) and were implemented using the SigmaPlot software. The computational effort is trivial, and practically zero computer time is involved. Figure 5 shows similar fits for the chemical agent HD at three experimental temperatures. The fitted diffusivity in air for both water and HD obtained from the simultaneous fit of volume and contact angle data is summarized in Table 1. For comparison, the diffusivities in air determined by the finite element simulations [13] and the predictions from FSG empirical correlation for diffusivities are also listed in Table 1. The diffusivities from the analytical approach for both water and HD are in good agreement with diffusivity estimates obtained by Willis et al. [13] using finite element simulations.

In addition to comparing our approximate analytical approach using the experimental data of Willis et al., our approach was also tested by conducting our own experiments on the evaporation of sessile drops of water on aluminum substrate. The sessile water droplet remained pinned with constant basal radius over the course of the experiment. From the experimental evaporation data at relative humidity of 39%, we estimate the diffusivity of water in air to be 2.0×10^{-5} m^2/s at 24 °C, which compares reasonably to the FSG equation estimate of 2.24×10^{-5} m^2/s at 24 °C (see the model fitting of volume and contact angle data in Supplemental Information S4).

To the best of our knowledge, this is the first time that volume and contact angle data were both simultaneously fitted to obtain estimates of diffusivity. Although the volume and contact angle are connected through the geometrical relations involving the basal radius, because of the difference between Eqs. (8) and (10) [Eq. (10) has additional contact angle-dependent term appearing in it compared to Eq. (8)], it is quite possible for the volume versus time and contact angle versus time to be fitted by differing diffusivity estimates. To confirm how well the approximate analytical approach works with other published data in the literature, we analyzed the classical

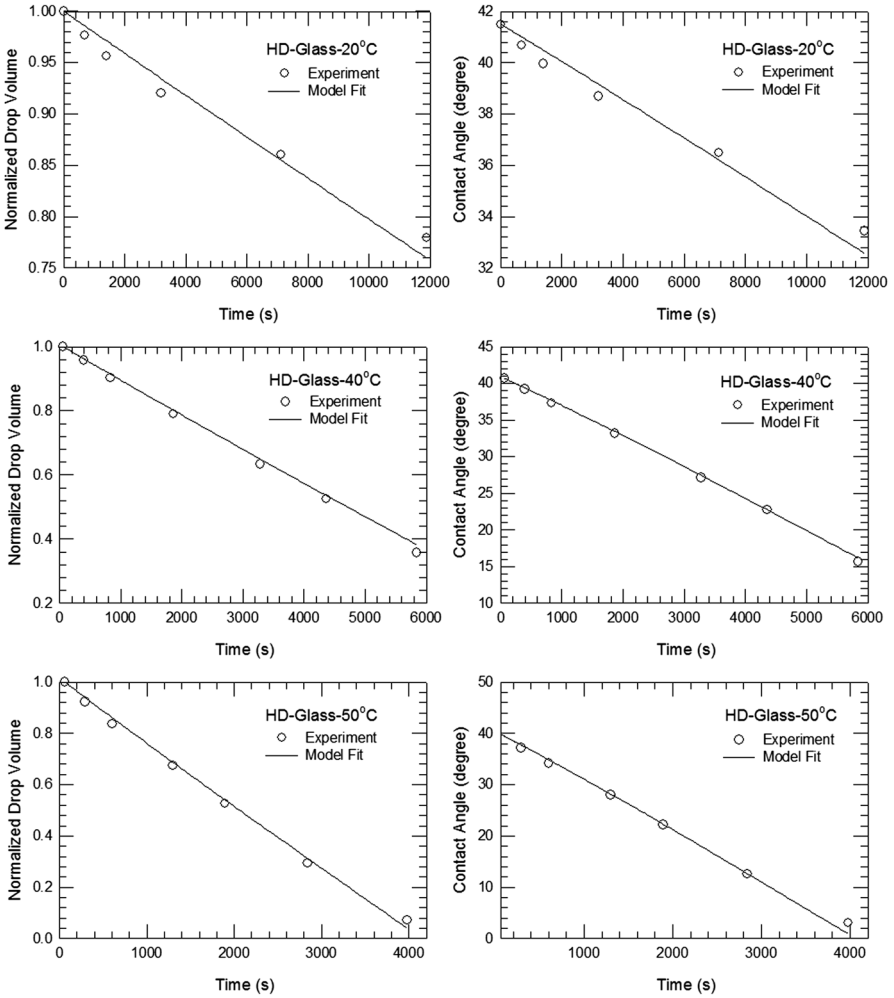

Fig. 5 Model fits of volume versus time and contact angle versus time data for HD on glass at three temperatures (20, 40, and 50 °C). The experimental data are from Willis et al. [13]

Table 1 Diffusivities in air (D_{SA}) for water and HD from evaporation experiments

Solvent	T (°C)	Analytical approach ($\times 10^{-5}$ m^2/s)	Finite element model [13] ($\times 10^{-5}$ m^2/s)	Estimate from FSG equation ($\times 10^{-5}$ m^2/s)
Water	20	2.1	2.4	2.2
Water	40	2.7	2.7	2.4
Water	60	3.2	3.2	2.6
HD	20	0.75	0.68	0.70
HD	40	0.84	0.79	0.78
HD	50	0.97	1.01	0.82

data gathered by Birdi et al. [3] using water droplets of three sizes to study evaporation into air. In that study, the mass of water remaining on the glass surface following evaporation was reported for water droplets of 5, 10, and 15 μL volume. In all cases, the initial contact angle was determined to be 41°. The diffusivity was estimated to be 1.85, 2.1, and 2.3×10^{-5} m^2/s for the droplets of size 5, 10, and 15 μL, respectively, taking the relative humidity for all experiments to be constant at 40% (see Supplemental Information S4 for details and for the fitting plots). We were able to fit both the contact angle and volume data simultaneously, for all three droplet sizes.

The approximate analytical approach for simultaneous evaporation/absorption was applied to the sessile drop volume versus time data reported by Willis et al. for HD on silicone substrate [12]. The normalized sessile drop volume versus time data for HD on silicone shown in Fig. 5 of Ref. [12] were used as the data for analysis. The actual volume of the sessile drop was kept close to, but not necessarily exactly at, the target volume of 1 μL in these experiments. Since the variation from the target volume was reported to be not large, the initial droplet volume was taken to be 1 μL for determining the actual volume versus time data. The $V(t)$ versus t data were converted to contact angle versus time data, using Eq. (4) for the spherical cap geometry, taking the basal radius to be constant and having the values 0.95, 1.025, and 1.10 mm at 20, 40, and 50 °C, respectively. Figure 6 shows the fits of experimental sessile drop volume versus time data to the integrated volume based on Eq. (13) and also the fits of the experimental sessile drop contact angle versus time data to the integrated contact angle based on Eq. (14) for HD on silicone substrate, at three temperatures.

The fits of data to the model at all three temperatures are quite good. The diffusivity in silicone for HD estimated from the simultaneous fit of both volume and contact angle data is summarized in Table 2. As discussed earlier, only the product $\phi_S^2 D_{SR}$ can be estimated by fitting the absorption data (Eqs. 13 and 14). To obtain an estimate for D_{SR}, the value of the partition coefficient ϕ_S must either be known or be obtained through independent equilibrium measurements. We have used the ϕ_S values of 0.1179, 0.1270, and 0.1357 at 20, 40, and 50 °C, respectively, reported in Ref. [12], to estimate the diffusivities from the analytical approach. For comparison, the diffusivities determined by the finite element simulations [12] are also listed in Table 2. Predictions for HD on silicone for all three temperatures, based on the simultaneous fitting of the volume and contact angle data, are in reasonable agreement with the finite element simulation results of Willis et al. [12].

Parametric sensitivity of diffusivity estimates to experimental variability

The estimation of diffusivity is entirely based on the measured values of contact angle and basal radius. Therefore, we assess how variations in these two experimental variables impact on the estimated diffusivity. For this purpose, we have used the data from Willis et al. [12] for HD on silicone substrate at 40 °C and have investigated the sensitivity of the model to experimental measurement variations. In Table 3, the basal radius (R_b) and contact angle (θ) are changed ± 10% from the experimental values and the diffusivity into silicone is estimated for all possible variations. R_b ratio and θ ratio specify the factors by which the experimental basal

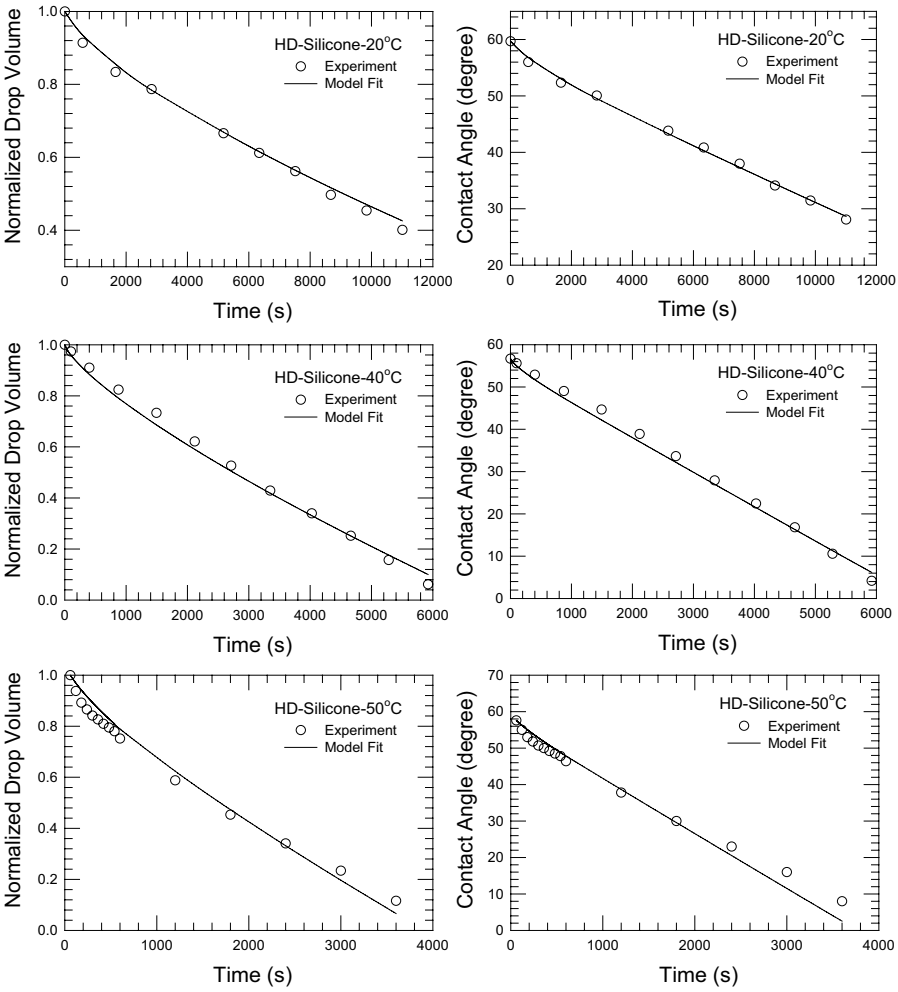

Fig. 6 Model fits of volume versus time and contact angle versus time for HD on silicone at three temperatures (20, 40, and 50 °C). The experimental data are from Willis et al. [12]

Table 2 HD absorption in silicone—comparison of diffusivities (D_{SR})

Temperature (°C)	ϕ_s	Analytical approach ($\times 10^{-10}$ m^2/s)	Finite element [12] ($\times 10^{-10}$ m^2/s)
20	0.1179	1.05	1.0
40	0.1270	1.9	2.1
50	0.1357	2.5	3.8

Table 3 Parametric sensitivity of diffusivity estimates on basal radius and contact angle variations for HD in silicone at 40 °C

R_b ratio	θ ratio	D_{SR} ($\times 10^{-10}$ m^2/s)
1	1	1.9
1.1	1	3.1
0.9	1	0.9
1	1.1	3.2
1	0.9	1.0
0.9	0.9	0.35
1.1	1.1	5.5
0.9	1.1	1.8
1.1	0.9	1.8

radius and contact angles have been altered. In all cases, the volume versus time and contact angle versus time were simultaneously fitted using the same diffusivity, and the results are summarized in Table 3.

Increasing basal radius or increasing contact angle has the same consequence, causing an increase in the estimate of diffusivity, D_{SR}. Similarly, decreasing either the basal radius or the contact angle decreases the diffusivity estimate. If either the basal radius or the contact angle increases while the other decreases, then the effects compensate and the diffusivity estimate is not modified. The largest changes in the diffusivity estimates arise when both the basal radius and the contact angle are increased or both are decreased. Taking the diffusivity estimate at R_b ratio = 1 and θ ratio = 1 as the reference or correct value, within this parametric space, the estimate for diffusivity D_{SR} is altered by a factor of 3–5 depending on the extent of errors in either the basal radius or the contact angle measurements. These calculations clearly suggest that good experimental measurements of contact angle and basal radius are needed for an accurate determination of diffusivity. At the same time, these calculations also show that a reasonably approximate estimate for diffusivity can be obtained by tolerating some experimental errors.

Assessing the domain of applicability of the sessile drop technique

The sessile drop technique for determining diffusivity in a solid is not viable for all liquids on all substrates. That is because liquid evaporation and absorption are simultaneous processes and a reliable estimation of diffusivity in the solid is possible only if the droplet mass loss by evaporation into air does not overwhelm the mass loss by absorption into the solid. The mass transport rates are controlled by the diffusivities as well as the concentration driving forces for evaporation and absorption, namely (P_S^*/P) and ϕ_s, respectively. Therefore, a simplified way to assess the relative importance of evaporation rate over absorption rate is to consider the ratio of the products of diffusivity and the driving force as below:

$$\frac{\text{evaporation}}{\text{absorption}} \propto \frac{D_{SA}(P_S^*/P)}{D_{SR}^{1/2}\phi_s}.$$

This ratio has been calculated for the HD–silicone system at the three experimental temperatures, and the results are summarized in Table S5—Supplemental Information S5. The evaporation-to-absorption ratio for HD at the three temperatures is 5.37×10^{-4}, 1.95×10^{-3}, and 2.92×10^{-3} m/s$^{1/2}$, respectively. To assess the domain of reliable use of the sessile drop technique in terms of the relative importance of evaporation and absorption, we should conduct experiments for systems where the evaporation-to-absorption ratio as defined above has increasingly larger values. Previous studies in our laboratory focused on the use of immersion technique for estimating the diffusivity into butyl rubber of several toxic chemicals [20]. Based on the results from that study, the relative evaporation-to-absorption ratio for these toxic chemicals could be estimated. Three chemicals, trichloroethylene, tetrachloroethylene, and acetonitrile, were chosen based upon their evaporation to absorption rate ratios of 4.3×10^{-2}, 1.09×10^{-1}, and 4.2 m/s$^{1/2}$ (details in Supplemental Information S5). These ratios are one to four orders of magnitude larger than the ratios for HD, and the major contribution to these large ratios comes from the high vapor pressures of the three selected chemicals.

Diffusivity estimates of three toxic chemicals from sessile drop measurements

Experimental data on contact angle and basal radius for the three toxic chemicals, trichloroethylene, tetrachloroethylene, and acetonitrile, were obtained from sessile drop profiles on aluminum substrate, when only evaporation occurs. The volume versus time and contact angle versus time are fitted to the approximate analytical approach in Fig. 7 to estimate the diffusivities in air. All three solvents have high vapor pressures as estimated from the Antoine equation, 0.022, 0.089, and 0.098 atm for tetrachloroethylene, trichloroethylene, and acetonitrile, respectively (compared to the values of 0.0001 to 0.001 atm for HD over the temperature range of 20–50 °C), which resulted in rapid evaporation into air. This is reflected in the much reduced timescale of these experiments compared to the experiments with HD on glass. The average evaporation rates estimated from the actual volume versus time measurements are approximately 0.36, 1.04, and 0.99 μL/min for tetrachloroethylene, trichloroethylene, and acetonitrile, respectively, compared to the average evaporation rates of 0.001, 0.006, and 0.014 μL/min for HD at 20, 40, and 50 °C.

For all three chemicals, we obtain good fit of volume versus time and contact angle versus time data, indicating that evaporation can be effectively followed by the sessile drop technique. For acetonitrile, the contact angle shows two regimes of behavior, one of decreasing contact angle and the other of constant contact angle. The contact angle decreases up to 20 s and then remains constant. The volume continues to decrease because after 20 s there is more change due to decreasing basal radius. This is a known phenomenon when there are stages in sessile droplet evaporation. In one phase the basal radius stays constant and contact angle decreases, and after a certain point the contact angle stays constant and the basal radius will decrease [5]. Volume versus time data can be used for the fitting over the entire time domain, but the contact angle fit can be used only in the domain where the contact angle is changing.

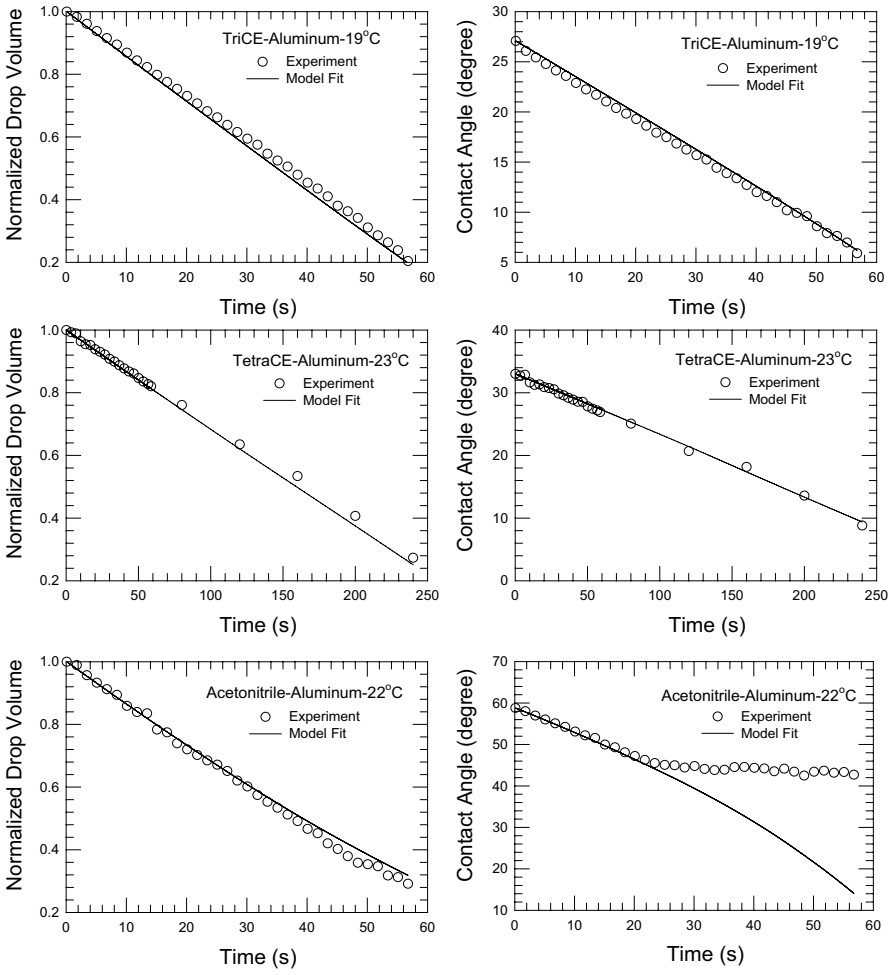

Fig. 7 Model fits of the volume versus time and contact angle versus time data for tetrachloroethylene (TetraCE), trichloroethylene (TriCE), and acetonitrile on aluminum at room temperature, as specified

The diffusivity estimates for acetonitrile, tetrachloroethylene, and trichloroethylene in air are summarized in Table 4. These values are compared against reported values in the literature as well as a prediction using the FSG equation. In the experiments involving these three chemicals, changes occur in the basal radius and these variations are of course taken into account in the model, as described earlier.

Experimental data on contact angle and basal radius for the three toxic chemicals were measured on butyl rubber substrate, when both evaporation and absorption simultaneously occur. The volume versus time and contact angle versus time are fitted to the approximate analytical approach in Fig. 8 to estimate their diffusivities in butyl rubber.

Table 4 Estimated values of solvent diffusivity in air (D_{SA})

Solvent	Analytical approach ($\times 10^{-6}$ m^2/s)	Experiments at 25 °C ($\times 10^{-6}$ m^2/s)	Estimate from FSG equation ($\times 10^{-6}$ m^2/s)
Tetrachloroethylene	9.8	7.11 [21] 7.97 [22]	7.7
Trichloroethylene	9.8	8.0 [21] 8.75 [22]	8.3
Acetonitrile	15.5	10.59 [22]	13.1

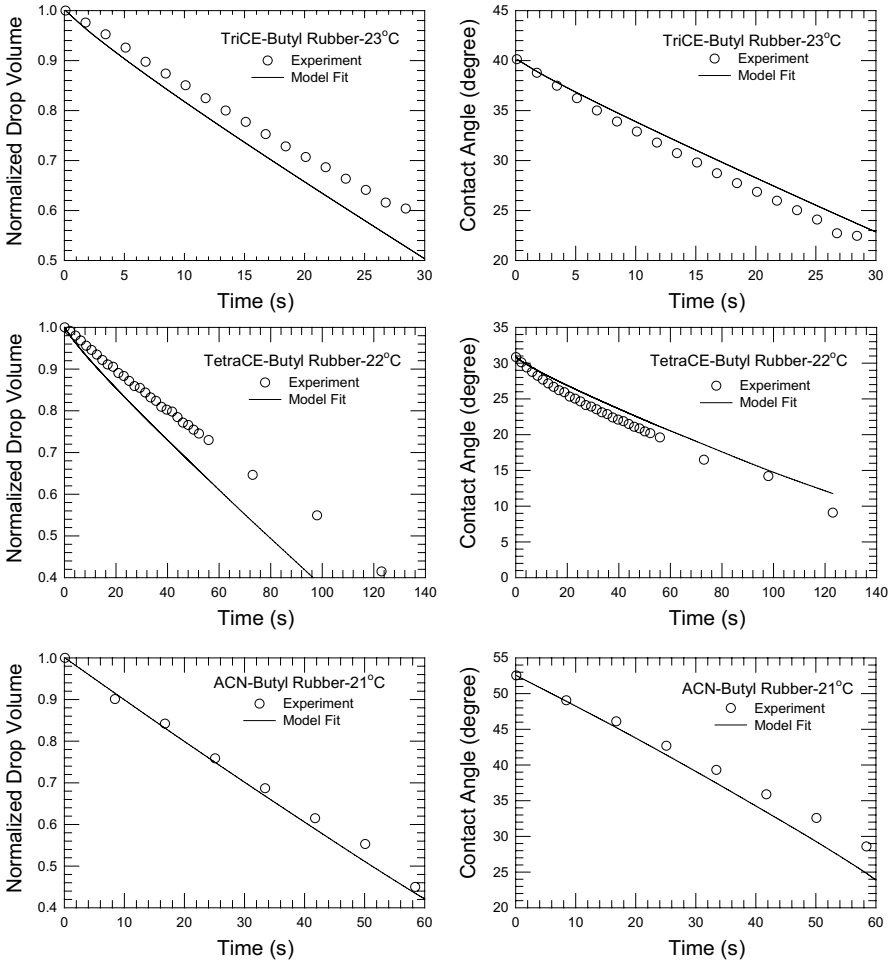

Fig. 8 Model fits of the tetrachloroethylene (TetraCE) and trichloroethylene (TriCE) on butyl rubber for volume versus time and contact angle versus time at room temperature, as indicated

The estimated values of D_{SA} in Table 4 were used in the evaporation/absorption model to obtain estimates of $\phi_S^2 D_{SR}$ for tetrachloroethylene and trichloroethylene in butyl rubber. As mentioned previously, in order to obtain estimates for the diffusion coefficient, D_{SR}, the equilibrium solvent volume fraction ϕ_S must be known. The equilibrium solvent volume fractions were determined in our previous work by immersion testing [20] to be 0.068, 0.717, and 0.717 for acetonitrile, tetrachloroethylene, and trichloroethylene, respectively. The resulting estimates for solvent diffusivity in butyl rubber, from the simultaneous fit of both volume and contact angle data (the model fit lines shown in Fig. 8) are listed in Table 5, along with the estimates obtained from immersion testing experiments. Also shown are the diffusivity estimates obtained for best fits if only the volume data or the contact angle data are considered instead of considering both volume and contact angle simultaneously.

The diffusivity of acetonitrile in butyl rubber could not be determined because evaporation by itself accounts for all the observed changes in volume and contact angle. We had calculated the relative evaporation to absorption ratios to be 4.3×10^{-2}, 1.09×10^{-1}, and 4.2 $m/s^{1/2}$ for tetrachloroethylene, trichloroethylene, and acetonitrile, respectively, compared to values of about 5×10^{-4} to 30×10^{-4} for HD at the three temperatures studied. The largest ratio is for acetonitrile, several orders of magnitude larger than that for HD, indicating that evaporation is significant even at the very early stages of the measurement process, preventing the determination of its diffusivity in butyl rubber.

For tetrachloroethylene and trichloroethylene, we observe from Fig. 8 that the diffusivity estimates from the simultaneous fit of both the volume versus time and contact angle versus time data do not show good fits of the kind shown in Fig. 6 for HD in silicone. Indeed, one could fit the volume and contact angle data for tetrachloroethylene and trichloroethylene very accurately to the model equations, by fitting each type of data independently. The different estimates of diffusivity for the same system, obtained from such independent fits, are also listed in Table 5. One can observe that the diffusivity estimate by fitting contact angle data is closer to the experimental estimate from the immersion method and the diffusivity estimate by fitting the volume data is always smaller.

The inability to fit both the volume and contact angle data simultaneously to a single diffusivity estimate accurately as well as the lower estimate from the fit of the volume data is a direct consequence of the high evaporation-to-absorption ratio

Table 5 Estimated values of solvent diffusivity in butyl rubber (D_{SR})

Solvent	Analytical approach ($\times 10^{-11}$ m^2/s)			Immersion experiments [20] ($\times 10^{-11}$ m^2/s)
	Fit shown in Fig. 8	Fit of volume data alone	Fit of contact angle data alone	
Tetrachloroethylene	1.0	0.2	2.5	3.2
Trichloroethylene	5.0	4.0	12.0	8.9
Acetonitrile	nd[a]	nd[a]	nd[a]	2.0

[a]Diffusivity could not be determined because evaporation by itself accounts for all the changes in volume and contact angle

for tetrachloroethylene and trichloroethylene. When the evaporation-to-absorption ratio is not so large, as in the case of HD, both volume and contact angle can be simultaneously fitted to obtain accurate diffusivity estimates. Compared to HD, the evaporation-to-absorption ratios are 10–100 times larger for tetrachloroethylene and trichloroethylene. When the evaporation-to-absorption ratio is large, the volume changes occurring as a result of sorption into the solid is much smaller than the volume changes occurring due to evaporation. Since the volume change is additive from the evaporation and absorption processes, when the volume change contribution from absorption is much smaller than that from evaporation, the diffusivity estimates from volume data become less reliable, typically becoming lower. In marked contrast, the contact angle which is also affected by both evaporation and absorption processes is not additive. Since the contact angle changes are not simply additive, the contact angle continues to capture the two processes more accurately even when the volume change due to absorption is very small compared to that due to evaporation. That is why the diffusivity estimates from the contact angle data are much closer to the experimental values, while those from the volume data are lower, for situations when the evaporation-to-absorption ratio is very large. When the evaporation mass losses totally overwhelm the absorption mass losses as in the case of acetonitrile, the estimation of diffusivity in the solid becomes impossible even with the use of the contact angle data.

Diffusivity of water in Nafion

We further explored the applicability of the sessile drop technique to a more complex polymer–solvent system by studying the sessile drop profiles of water on a Nafion membrane, where the water sorption is known to swell the membrane. Nafion has been extensively explored for use as an ion conducting membrane in fuel cell applications. Nafion-like membranes are also considered as viable candidates for protective clothing providing barrier against chemical threat agents while allowing for moisture transport. Nafion is a copolymer with a hydrophobic backbone of tetrafluoroethylene, with side chains containing strongly hydrophilic sulfonic acid groups. It is believed that there is microphase separation between hydrophilic and hydrophobic groups giving rise to unusual physical and mechanical properties. The microstructure of Nafion is envisioned as sulfonic acid groups that cluster to form a hydrophilic microphase surrounded by a continuous hydrophobic tetrafluoroethylene phase. Water is absorbed into the hydrophilic domains solvating the acid groups causing the polymer to swell.

We imaged the sessile drop profiles of water on a Nafion 1100 membrane at 22 °C and relative humidity of 23%. Figure 9 shows the simultaneous fit of both volume–time and contact angle–time data to the analytical model using a common diffusion coefficient. The fit is reasonable, but one can observe that the specific profile of the contact angle versus time data is not reflected by the model fit. We believe this is due to the swelling effects on the membrane and the simple representation by Eq. (11) for the absorption of liquid by the polymer used in our model does not cover this physical phenomenon.

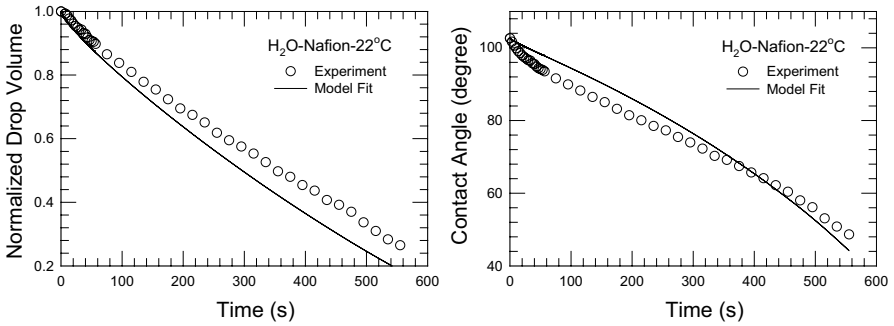

Fig. 9 Model fits of volume versus time and contact angle versus time for water on Nafion 1100 at 22 °C

We have used the water diffusivity in air estimated in this study (approximately 2.1×10^{-5} m^2/s at 22 °C) while fitting the simultaneous evaporation and absorption data for water on Nafion membrane shown in Fig. 9. As discussed earlier, only the product $\phi_S^2 D_{SR}$ can be estimated by fitting the evaporation/absorption data through Eqs. (13) and (14). To obtain an estimate for D_{SR}, the value of the partition coefficient ϕ_S must either be known or be obtained through independent equilibrium measurements. Reasonably good fits for both volume and contact angle data are obtained for assumed ϕ_S values of 0.2, 0.4, and 0.6 and the corresponding diffusivity estimates of 5×10^{-10}, 2×10^{-10}, and 1×10^{-10} m^2/s, respectively. The fit shown in Fig. 9 corresponds to a ϕ_S value of 0.4 and the corresponding diffusivity estimate of 2×10^{-10} m^2/s. A range of diffusivity values from 0.8×10^{-10} and 8.0×10^{-10} m^2/s a have been reported in the literature based on experiments with liquid water and various Nafion membranes, in the temperature range of 20–30 °C and using different experimental techniques, as summarized in Ref. [23]. In that study, using a Nafion 117 membrane, for water activity close to 1, the ϕ_S value of about 0.32 and diffusivity estimates of 1.3×10^{-10} and 1.6×10^{-10} m^2/s are reported. The estimate for diffusivity and the assumed saturation volume fraction of water in Nafion based on our measurements are within the range of these reported experimental data in the literature.

Relative absorption and evaporation rates and recommendation of solvents for barrier studies

We considered earlier the ratio of evaporation to absorption represented by the product of diffusivity and the concentration driving force:

$$\frac{\text{evaporation}}{\text{absorption}} \propto \frac{D_{SA}(P_S^*/P)}{D_{SR}^{1/2}\phi_s}$$

as a relative measure to compare various solvent–solid systems. The actual evaporation and absorption rates can be calculated from the two terms appearing in

Eq. (13). The first term represents the volume rate of change due to evaporation, while the second represents the same for absorption. The ratios between these calculated absorption and evaporation rates as a function of time are shown in Fig. 10 for all solvent–solid systems considered in this study. The figure also includes the actual magnitude of the rate of volume change due to evaporation as a function of the total rate of volume change due to both evaporation and absorption. In general, absorption rates are relatively large at early times and they decrease as time increases. The rate of absorption remains larger than the rate of evaporation over a significant time range for HD on silicone at all three temperatures and also for water on Nafion. The absorption rate is always smaller than that of the evaporation rate for tetrachloroethylene and trichloroethylene, and indeed, the ratio of absorption to evaporation rate falls rapidly over a short time interval. The absolute evaporation rates for trichloroethylene and tetrachloroethylene are orders of magnitude large than that for HD. These comparative rates help explain why it is possible to get accurate estimates for diffusivities by fitting both volume and contact angle data for some systems, but how this becomes challenging for others.

Based on these rate assessments, we can identify solvents that could be considered good candidates for evaluating barrier materials for chemical agent protection applications. The key variable contributing to the high evaporation-to-absorption ratio is the vapor pressure of the solvent. Therefore, for any new barrier materials, it would be safe to conduct sessile drop experiments using solvents that have low vapor pressures. A compilation [24] of many simulants for chemical agents is available, which also lists the vapor pressures of agents and the simulants. One can identify a number of simulants for the chemical agents from this compilation if one wants to adopt the sessile drop technique to screen new barrier materials.

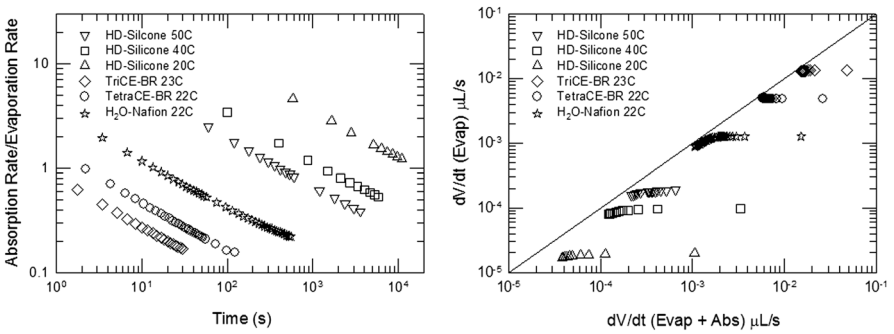

Fig. 10 Comparing absorption and evaporation rates for HD on silicone for three temperatures (20, 40, and 50 °C), trichloroethylene and tetrachloroethylene on butyl rubber, and water on Nafion. Left—ratio of absorption rate to evaporation rate versus time. Right—rate of change of volume due to evaporation versus rate of change of volume due to both evaporation and absorption

Conclusions

We have demonstrated that a simple approximate analytical model is adequate to extract diffusivity data for liquids in solids from experimentally determined time evolution of sessile drop profiles. The contact angle and basal radius determined from the sessile drop profile can be used to calculate also the drop volume versus time data. Both the volume versus time and contact angle versus time data can be simultaneously fitted to the approximate analytical equation to estimate the diffusivity of the liquid in the solid. The approach is computationally trivial and therefore can serve as a fast screening method for evaluating new barrier materials. This approach can be used over the domain where the contact angle changes with time, but not where the contact angle remains constant, as shown by acetonitrile data on aluminum. In this case, the volume data over the entire time domain can still be used to obtain diffusivity.

The main limitation of the sessile drop technique is that it cannot provide reliable diffusivity estimates (within small bounds) when the solvent is significantly volatile such that the rate of absorption into the solid is much smaller than the rate of evaporation into air. We show that even when the evaporation-to-absorption ratio is large as in the case of trichloroethylene and tetrachloroethylene, the contact angle data can be reliably used to get the diffusivity in the solid. Only when the ratio becomes too large as in the case of acetonitrile, that diffusivity estimation by this method becomes not possible. Through the assessment of the relative rates of absorption and evaporation and by conducting experiments, we concluded that solvents with lower vapor pressures would be ideal candidates for use with the sessile drop technique. One approach to eliminating this constraint on the selection of solvents is to eliminate or reduce the evaporation rate by conducting the experiments in air saturated with the solvent vapor. However, this may not be needed for practical applications since many simulants for chemical warfare agents, having low vapor pressures, are available. The sessile drop technique with drop volumes of ~ 1 μL can definitely provide reasonably accurate estimates for diffusivity in solid barrier materials, based on experiments that take only 1–10 min and requiring only trivial computational effort.

Acknowledgements This work was supported by Defense Threat Reduction Agency (Project BA10PHM050) and Natick Soldier Research, Development and Engineering Center. Research was performed while MNR, MB, and RS held an Oak Ridge Institute for Science and Education (ORISE) Fellowship. We acknowledge helpful discussions with Dr. Matthew Willis and Dr. Brent Mantooth of Edgewood Chemical and Biological Center about their work described in References [12] and [13].

Funding The research was supported by U. S. Defense Threat Reduction Agency (Project BA10PHM050) and Natick Soldier Research, Development and Engineering Center.

Compliance with ethical standards

Conflict of interest The authors declare that they have no conflict of interest.

References

1. Aiial US, Aminabhavi TM (1990) Measurement of diffusivity of organic liquids through polymer membranes: a simple and inexpensive laboratory experiment. J Chem Educ 67:82–85. https://doi.org/10.1021/ed067p82
2. Picknett RG, Bexon R (1977) The evaporation of sessile or pendant drops in still air. J Colloid Interface Sci 61:336–350. https://doi.org/10.1016/0021-9797(77)90396-4
3. Birdi KS, Vu DT, Winter A (1989) A study of the evaporation rates of small water drops placed on a solid surface. J Phys Chem 93:3702–3703. https://doi.org/10.1021/j100346a065
4. Rowan SM, Newton MI, McHale G (1995) Evaporation of microdroplets and the wetting of solid surfaces. J Phys Chem 99:12268–12271. https://doi.org/10.1021/j100035a034
5. Bourges-Monnier C, Shanahan MER (1995) Influence of evaporation on contact angle. Langmuir 11:2820–2829. https://doi.org/10.1021/la00007a076
6. Hu H, Larson RG (2002) Evaporation of a sessile droplet on a substrate. J Phys Chem B 106:1234–1244. https://doi.org/10.1021/jp0118322
7. Cazabat AM, Guéna G (2010) Evaporation of macroscopic sessile droplets. Soft Matter 6:2591–2613. https://doi.org/10.1039/b924477h
8. Song H, Lee Y, Jin S, Kim HY, Yoo JY (2011) Prediction of sessile drop evaporation considering surface wettability. Microelectron Eng 88:3249–3255. https://doi.org/10.1016/j.mee.2011.07.015
9. Nguyen TAH, Nguyen AV, Hampton MA, Xu ZP, Huang L, Rudolph V (2013) Theoretical and experimental analysis of droplet evaporation on solid surfaces. Chem Eng Sci 69:522–529. https://doi.org/10.1016/j.ces.2011.11.009
10. Stauber JM, Wilson SK, Duffy BR, Sefiane K (2015) On the evaporation of droplets on strongly hydrophobic substrates. Langmuir 31:2353–2360. https://doi.org/10.1021/acs.langmuir.5b00286
11. Erbil HY (2013) Evaporation of pure liquid sessile and spherical suspended drops: a review. Adv Colloid Interface Sci 170:67–86. https://doi.org/10.1016/j.cis.2011.13.006
12. Willis MP, Mantooth BA, Lalain TA (2013) Novel methodology for the estimation of chemical warfare agent mass transport dynamics. Part II: absorption. J Phys Chem C 116:546–554. https://doi.org/10.1021/jp2087847
13. Willis MP, Mantooth BA, Lalain TA (2013) Novel methodology for the estimation of chemical warfare agent mass transport dynamics, part I: evaporation. J Phys Chem C 116:538–545. https://doi.org/10.1021/jp2087835
14. Kelly-Zion PL, Batra J, Pursell CJ (2013) Correlation for the convective and diffusive evaporation of a sessile drop. Int J Heat Mass Transfer 64:278–285. https://doi.org/10.1016/j.ijheatmasstransfer.2012.04.051
15. Extrand CW, Moon SI (2010) When sessile drops are no longer small: transitions from spherical to fully flattened. Langmuir 26:11815–11822. https://doi.org/10.1021/la1005123
16. Bird RS, Stewart W, Lightfoot E (1960) Transport Phenomena. Wiley, New York
17. Crank J (1979) The mathematics of diffusion. Clarendon Press, Oxford
18. Reid RC, Prausnitz JM, Sherwood TK (1977) The Properties of gases and liquids. McGraw-Hill Book Company, New York
19. Fuller EN, Schettler PD, Giddings JC (1966) A new method for prediction of binary gas—phase diffusion coefficients. Ind Eng Chem 58:19–27. https://doi.org/10.1021/ie50677a007
20. Srinivasan S, Lavoie J, Nagarajan R (2014) Data-driven property estimation for protective clothing; US Army Natick Solider RD&E Center: Natick/TR-14/021
21. Watts H (1971) Temperature dependence of the diffusion of l,2 dichloroethane, l, l, l-trichloroethane, trichloroethylene, and tetrachloroethylene in air. Can J Chem 49:1965–1967. https://doi.org/10.1139/v71-316
22. Lugg GA (1968) Diffusion coefficients of some organic and other vapors in air. Anal Chem 40:1072–1077. https://doi.org/10.1021/ac60263a006
23. Onishi LM, Prausnitz JM, Newman J (2012) Steady-state diffusion coefficients for water in Nafion in the absence of inert gas. J Electrochem Soc 159:754–760. https://doi.org/10.1149/2.114206jes
24. Bartelt-Hunt SL, Knappe DRU, Barlaz MA (2008) A review of chemical warfare agent simulants for the study of environmental behavior. Crit Rev Environ Sci Technol 38:112–136. https://doi.org/10.1080/10643380701643650

An approximate analytical approach to estimate the diffusivity of toxic chemicals in polymer barrier materials from the time-evolution of sessile drop profiles

Polymer Bulletin

Supplementary Material

Molly N. Richards[1], Michael Bell[2], Rajagopalan Srinivasan[1], Ali Borhan[3], and Ramanathan Nagarajan[1*]

[1]Natick Soldier Research, Development and Engineering Center, Natick MA 01760

[2]Penn State University, Department of Physics, University Park, PA 16802

[3]Penn State University, Department of Chemical Engineering, University Park, PA 16802

*Corresponding Author Information

Natick Soldier Research, Development & Engineering Center (NSRDEC)

15 General Greene Avenue

Natick, MA 01760

Phone: 508-233-6445

E-mail: Ramanathan.nagarajan.civ@mail.mil

S1. Calculation of Bond number and critical volume where gravity force influences drop shape from that of spherical cap

Bond number is defined as $B_o = \rho g R_o^2/\gamma$, where ρ is the mass density of the liquid, g is the gravitational acceleration (9.8 m/s^2), R_0 is the equivalent-spherical radius of the droplet, and γ is the air-liquid surface tension. For 1 µl droplet, the radius of the sphere of equivalent volume is R_o = 0.620 x 10^{-3} m.

The critical volume V_c at which the gravity force causes distortions from spherical cap shape were estimated using the following equation provided by Extrand *et al* [1]:

$$V_c = \frac{1}{48}\pi\left(\frac{\gamma}{\rho g}\right)^{\frac{3}{2}} \tan\left(\frac{\theta}{2}\right)\left(3+\tan^2\frac{\theta}{2}\right)\left[\left(1+8\frac{\sin^2\theta}{1-\cos\theta}\right)^{1/2}-1\right]^3$$

where, γ is the surface tension of the liquid, ρ its density, θ is its contact angle on the surface and g is the acceleration due to gravity. In the Table below, the contact angle values given are those from our measurements on aluminum foil and butyl rubber sheet.

Table S1. Physical Properties and calculation of bond number and critical volume for tetrachloroethylene, trichloroethylene, and acetonitrile

Chemical	Surface Tension γ (N/m)	Mass density ρ (kg/m^3)	Bond Number	Contact Angle θ (degrees)		Critical Volume V_c (µL)	
				Al Foil	Butyl rubber	Al Foil	Butyl rubber
Tetrachloro ethylene	0.0317 [2]	1620	0.193	32	34	4.27	4.48
Trichloro ethylene	0.0293 [3]	1460	0.188	29	29	4.10	4.10
Acetonitrile	0.0293 [4]	786	0.101	58	51	16.08	15.22

References:

1. Extrand CW, Moon SI (2010) When sessile drops are no longer small: Transitions from spherical to fully flattened. Langmuir 26: 11815-11822. https://doi.org/10.1021/la1005133
2. Weast RC, Editor (1987-1988) Handbook of Chemistry and Physics, 68th Edition, CRC Press Inc, Boca Raton, Florida. p. F-37
3. U.S Cost Guard, Department of Transportation (1984-1985) CHRIS – Hazardous Chemical Data, Volume II, Government Printing Office, Washington DC.
4. O'Neil MJ, Editor (2013) The Merck Index - An Encyclopedia of Chemicals, Drugs, and Biologicals. Royal Society of Chemistry, Cambridge, UK. p. 14

S2. Antoine constants and Diffusion volumes for solvents investigated

Table S2. Molecular Properties of Solvents Investigated

Solvent	Mol. Wt.	Antoine A	Antoine B	Antoine C	Density (at T°C) g cm^{-3}	Diffusion Volume $\Sigma V_{S,atom}$ cm^3/mol
Acetonitrile CH_3CN	41.05	7.07	1279.2	224.01	1.282 (22)	44.63
Tetrachloroethylene $Cl_2C=CCl_2$	165.8	7.02	1415.5	221.01	1.623 (22)	111
Trichloroethylene $Cl_2C=CHCl$	131.4	7.03	1315.1	230.01	1.460 (22)	93.48
Water H_2O	18	8.07	1730.6	233.43	0.998 (20) 0.992 (40) 0.983 (60)	12.7
Mustard, HD $(ClCH_2CH_2)_2S$	159.1	7.47	1935.5	204.2	1.274 (20) 1.253 (40) 1.242 (50)	129.2

*Diffusion volumes were calculated using atomic group contributions in Table 11-1 of Ref [1]. The Antoine constants and liquid density data are from Ref [1] for water, acetonitrile, tetrachloroethylene and trichloroethylene and from Ref [2] for HD

References:

1. Reid RC, Prausnitz JM, Sherwood TK (1977) The Properties of Gases and Liquids: McGraw-Hill Book Company: New York.

2. Willis MP, Mantooth BA, Lalain TA (2013) Novel methodology for the estimation of chemical warfare agent mass transport dynamics, Part I: Evaporation. J Phys Chem C 116: 538-545. https://doi.org/10.1021/jp2087835

S3. Integration to determine volume and contact angle as a function of time.

For simultaneous evaporation and absorption, the rates of change of volume and contact angle are given by Eqs.(13) and (14) in the text.

$$\frac{dV}{dt} = -\alpha R_b(0.27\theta^2 + 1.30) - \pi R_b^2 \phi_S \left(\frac{D_{SR}}{\pi t}\right)^{1/2} \tag{13}$$

$$\frac{d\theta}{dt} = -\frac{4}{\pi R_b^2}\cos^4(\frac{\theta}{2}) \left[\alpha\,(0.27\theta^2 + 1.30) + \pi R_b \phi_S \left(\frac{D_{SR}}{\pi t}\right)^{1/2}\right] \tag{14}$$

For the case of evaporation alone, the second term in the above two equations are excluded. From the experiments, we measure θ and R_b at various times t and we calculate the corresponding volume V using Eq.(4). The integrations are then performed as simple summations from the table of experimental data. For the i[th] data from the experiment,

$$\frac{\Delta V_i}{\Delta t_i} = -\alpha R_{bi}(0.27\theta_i^2 + 1.30) - \pi R_{bi}^2 \phi_S \left(\frac{D_{SR}}{\pi t_i}\right)^{1/2}$$

$$\frac{\Delta \theta_i}{\Delta t_i} = -\frac{4}{\pi R_b^2}\cos^4(\frac{\theta_i}{2}) \left[\alpha\,(0.27\theta_i^2 + 1.30) + \pi R_{bi} \phi_S \left(\frac{D_{SR}}{\pi t_i}\right)^{1/2}\right]$$

$$V_i = V_o + \sum_{i=1}^{i} \frac{\Delta V_i}{\Delta t_i}\,\Delta t_i \;, \qquad \theta_i = \theta_o + \sum_{i=1}^{i} \frac{\Delta \theta_i}{\Delta t_i}\,\Delta t_i \;\;,\;\; \Delta t_i = t_i - t_{i-1}$$

The instantaneous θ_i and V_i measured at various times t_i are fitted to the summations above (which are the calculated instantaneous values of volume and contact angle) to obtain the diffusivity as the fitted parameter. The time intervals for integration or integration methods are not critical to the results obtained.

The calculations (involves only summations) were done using SigmaPlot but any common software including EXCEL will be more than adequate.

S4. Analysis of additional water evaporation data

Water evaporation measurements were made in our laboratory by imaging sessile drops of water on aluminum substrate undergoing evaporation. The contact angle and basal radius were measured as functions of time. The sessile water droplet remained pinned with constant basal radius over the course of the experiment. The experimental temperature was 24ºC and the ambient relative humidity was 39%. From the time-dependent contact angle and basal radius, the experimental volume vs time data were calculated. The experimental volume vs time and contact angle vs time data were simultaneously fitted as shown below in Figure S3-1 to yield an estimate for the diffusivity of water in air to be 2.0 x 10^{-5} m^2/s at 24ºC

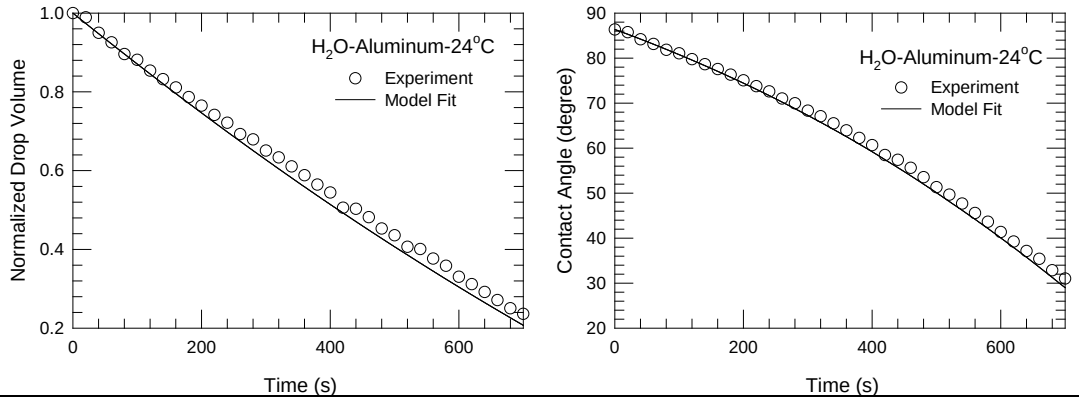

Figure S3-1. Simultaneous fitting of experimental normalized volume and contact angle data to the approximate analytical model for the determination of diffusivity of water in air.

We further analyzed the classical evaporation data gathered by Birdi et al [1] using water sessile drops of three sizes to study evaporation into air. In that study, the mass of water remaining on a glass surface during evaporation was reported for water droplets of initial mass 5, 10 and 15 mg, respectively as a function of time. In all cases, the initial contact angle was determined to be 41º. From the initial volume of the droplet (calculated from the mass) and the initial contact angle, the initial basal radius was calculated using eq. (4) to be 2.01 mm, 2.53 mm and 2.9 mm, respectively. The basal radius was found to remain constant in that study. Using the time evolution of the mass of droplet data plotted in Figure 1 of Ref.[1], and the calculated basal radii, we calculated the volume vs time and contact angle vs time data for each of the droplet sizes. We then fitted them simultaneously as shown on Figure S3-2 below to obtain estimates of diffusivity in air. Since ref.[1] did not mention the relative humidity during the experiments but only mentioned that relative humidity was constant, we have fitted the data assuming a relative humidity of 40% as the corresponding diffusivity estimates would be comparable to other known measurements. Our goal here is not the determination of diffusivity values but only to examine that both volume and contact angle data can be simultaneously fitted with a single diffusivity value.

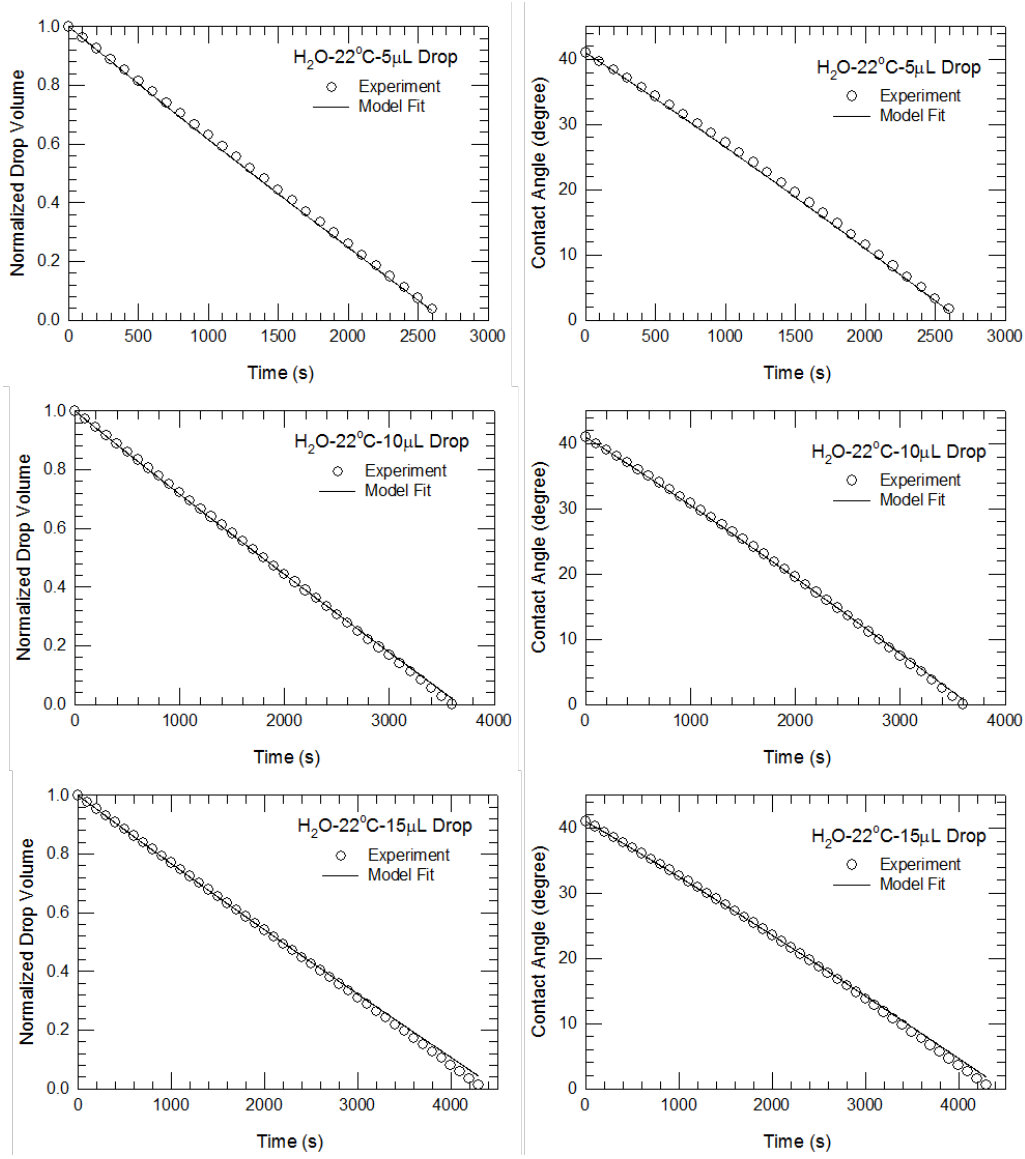

Figure S3-2. Simultaneous fitting of approximate analytical model to the volume vs. time and contact angle vs. time data for sessile drop measurements reported by Birdi, et al. [1] with droplets of different initial volumes.

References:

1. Birdi KS, Vu DT, Winter A (1989) A study of the evaporation rates of small water drops placed on a solid surface. J Phys Chem 93: 3702-3703. https://doi.org/10.1021/j100346a065

S5. Relative Evaporation and Absorption Mass Transfer Rates

The relative rate of evaporation to absorption is calculated in units in which each of the variable is represented in the table below.

Table S5. Variable of importance to mass transport and calculation of relative evaporation and absorption mass transfer rates

Solvent/ Substrate	T (^oC)	P_S^*/P[(a)]	ϕ_s[(b)]	D_{SA}[(c)] (m^2/s)	D_{SR}[(d)] (m^2/s)	$\frac{D_{SA}(P_S^*/P)}{{D_{SR}}^{1/2}\phi_s}$ ($m/s^{1/2}$)
HD Silicone	20	0.904×10^{-4}	0.1179	0.70×10^{-5}	1.0×10^{-10}	0.000537
HD Silicone	40	4.61×10^{-4}	0.1270	0.78×10^{-5}	2.1×10^{-10}	0.001954
HD Silicone	50	9.44×10^{-4}	0.1357	0.82×10^{-5}	3.8×10^{-10}	0.002926
Tetrachloro-ethylene Butyl rubber	22	0.0218	0.717	0.77×10^{-5}	0.32×10^{-10}	0.041386
Trichloro-ethylene Butyl rubber	22	0.089	0.717	0.83×10^{-5}	0.89×10^{-10}	0.109208
Acetonitrile Butyl rubber	22	0.0976	0.068	1.31×10^{-5}	0.20×10^{-10}	4.204334

[(a)]Vapor pressure calculated from Antoine equation using parameters listed in main text, Table S1

[(b)]Saturation volume fractions for HD from ref [1] and for other chemicals from ref [2]

[(c)]Diffusivity in air calculated from the FSG equation listed in main text, Tables 1 and 4

[(d)]Diffusivity in solid for HD from ref [1] and for other chemicals from ref [2]

References:

1. Willis MP, Mantooth BA, Lalain TA (2103) Novel methodology for the estimation of chemical warfare agent mass transport dynamics. Part II: Absorption. J Phys Chem C 116: 546-554. https://doi.org/10.1021/jp2087847
2. Srinivasan S, Lavoie J, Nagarajan R (2014) Data-Driven Property Estimation for Protective Clothing; US Army Natick Solider RD&E Center: Natick/TR-14/021